small
NANO MICRO

Fiber-Assisted Molding (FAM) of Surfaces with Tunable Curvature to Guide Cell Alignment and Complex Tissue Architecture

Vahid Hosseini, Philip Kollmannsberger, Samad Ahadian, Serge Ostrovidov, Hirokazu Kaji, Viola Vogel, and Ali Khademhosseini**

Nature has evolved a variety of highly efficient tissue and organ structures that are adapted to meet different functional requirements.[1] These structures are assembled and remodeled during growth and regeneration by cells that continuously interact with each other and the environment.[2] To better understand and reconstitute these processes, it is necessary to fabricate artificial culture substrates that closely mimic the environment that cells sense and respond to during tissue growth and regeneration.[3] Many techniques to produce geometrical structures with nano- to micrometer precision are available and have been successfully used to study the impact of substrate topography and geometry from nanometer to millimeter scales on cell alignment, migration, differentiation and matrix production.[4] Many of these techniques, however, suffer from high cost, complexity, poor scalability and the need for expensive and special equipment, such as clean room facilities, which poses limitations on their widespread applications. More importantly, most microfabrication techniques available today can only produce smaller sized structures with flat sides and sharp angles which are rarely seen in organs and tissues. Typical biological structures are composed of curved, tubular and sometimes helical surfaces on micro- to millimeter scales. Reproducing such structures and using them as cell culture substrates enables the in vitro recapitulation of the growth and adaptation processes that gives rise to complex functional tissue and organ architectures. A number of researchers have adapted existing or presented new unconventional fabrication methods to overcome the limitations of classical approaches. Sinusoidal wavy microgrooves with sizes of a few micrometer have been prepared by extensive, low pressure plasma oxidation of stretched poly (dimethylsiloxane) (PDMS) slabs.[5] This method however is unable to make large wavy structures and suffers from poor control over curvature and feature size. In another study, rounded microgrooves were made by plasma etching and oxide deposition over square profile grooves.[6] These curved grooves were successfully employed to align mammalian cells, showing the same effect on cell alignment as parallel micro- and nano-grooves created by conventional photolithographic approaches.[7] Recent advances in three-dimensional (3D) printing can be used to create complex shapes

V. Hosseini, Dr. P. Kollmannsberger, Prof. V. Vogel
Laboratory of Applied Mechanobiology
Department of Health Sciences and Technology
ETH Zurich, Vladimir-Prelog-Weg 1-5/10
CH-8093, Zurich, Switzerland
E-mail: viola.vogel@hest.ethz.ch

Prof. A. Khademhosseini, Dr. S. Ahadian, Dr. S. Ostrovidov
WPI-Advanced Institute for Materials Research
Tohoku University
Sendai 980–8577, Japan

Prof. H. Kaji
Department of Bioengineering and Robotics
Graduate School of Engineering
Tohoku University
Sendai 980–8579, Japan

Prof. A. Khademhosseini
Department of Medicine
Center for Biomedical Engineering
Brigham and Women's Hospital
Harvard Medical School
Cambridge, Massachusetts 02139, USA
E-mail: alik@rics.bwh.harvard.edu

Prof. A. Khademhosseini
Harvard-MIT Division of Health
Sciences and Technology
Massachusetts Institute of Technology
Cambridge, Massachusetts 02139, USA

Prof. A. Khademhosseini
Wyss Institute for Biologically Inspired Engineering
Harvard University
Boston, Massachusetts 02115, USA

Prof. A. Khademhosseini
Department of Maxillofacial Biomedical Engineering
and Institute of Oral Biology
School of Dentistry
Kyung Hee University
Seoul, Republic of Korea

Prof. A. Khademhosseini
Department of Physics
King Abdulaziz University
Jeddah 21569, Saudi Arabia

DOI: 10.1002/smll.201400263

and geometries on different length scales, however most 3D printers assemble 3D features from two-dimensional (2D) stacks with sizes on the order of tens of micrometers, which leads to step artifacts depending on the printer resolution.[8] Therefore, there is a continued need for the creation of controlled curvature without step defects.

Here, we introduce FAM as a simple yet versatile method to fabricate microgrooves with defined concave or convex curvature, sinusoidal grooves, parallel groove-patterned tubes, and double- and multiple-strand 3D helical structures (**Figure 1**). Commercially available nylon or metal threads of different diameters, here ranging from 100 µm to 500 µm,

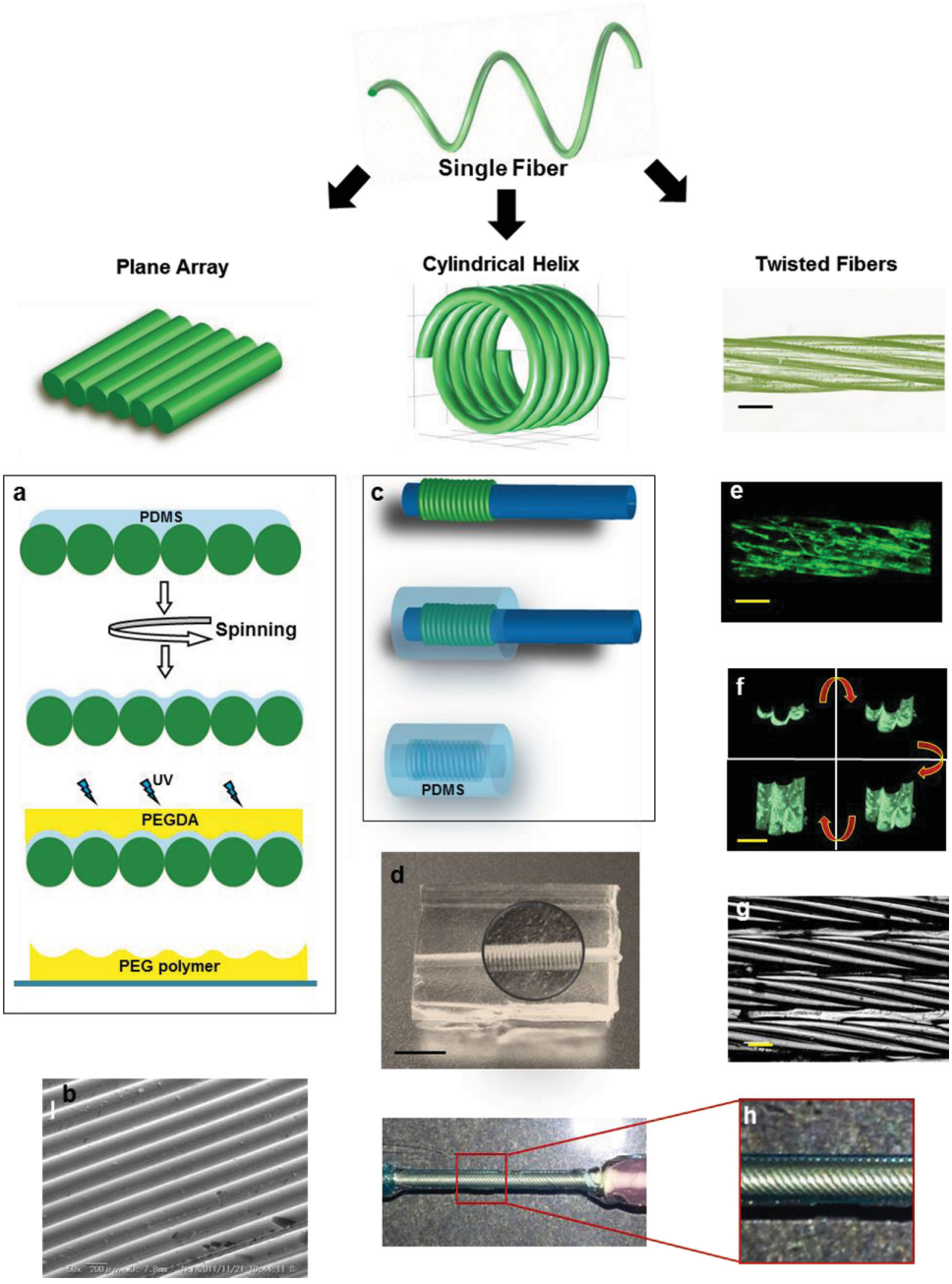

Figure 1. Schematics of the fiber-assisted molding (FAM) procedure and micrographs of different fiber templates. Producing planar arrays of wrapped fibers, helical fiber cylinders or twisted fibers. a) PDMS is puored over the fibers and centrifuged to remove excess PDMS. PEGDA prepolymer was added and then UV polymerized to create a permanent mold for replicating patterns in PDMS. b) SEM image of a PDMS mold made from PEG polymer template. Micropatterning of parallel grooves inside a tube. c) Three simple steps to create a hollow PDMS tube with a parallel micropattern inside by a single fiber and d) final PDMS construct with hollow tube patterned inside. The inner tube diameter is 0.5 mm; the outer diameter is 0.9 mm. Helical tube-like structure made by twisting fibers, e) 3D Z projection of human fibroblasts' fibrillar fibronectin matrix inside the tube following the helical pattern using twisted fiber template and f) part of the helical tube stained with FITC rotated 90° along the *x* axis for better illustration of the tube profile. g) Phase contrast image of parallel microgrooves in PDMS with helical pattern inside of each groove. h) Bundle of fibers wrapped helically around syringe needle to control the twisting angle, needle diameter is 1.2 mm and fiber diameter is 200 µm. Scale bars, 5 mm (d) and 200 µm (b,e–g).

small 2014,
DOI: 10.1002/smll.201400263

NANO MICRO small

were used to create the templates. The radius of curvature can easily be tuned by adjusting the fiber diameter. These templates were then used as substrate to culture and align fibroblasts and myoblasts on different curvatures and on helical structures. Fiber fabrication and assembly has recently gained attention for applications such as twisted capacitors and batteries,[9] solar cell optical fibers[10] and actuator muscles[11] but has not yet been utilized for biological applications. Electrospun fibers,[12] drawn parallel thread,[13] or single glass fibers[14] have all been used to align cells on flat substrates, but complex defined 3D curvature and wavy features were hard to achieve before. Our novel and simple approach establishes a new tool to study cells in complex helical and curved structures and opens up new possibilities to engineer human and animal tissues such as vessels, muscle, tendon, and neural tissue.

To create a wavy or semicircular groove pattern on planar or tubular geometries, primary fiber masters were prepared by wrapping a fiber or thread around a glass slide or a tube such as a syringe needle. We avoided using sharp-edged objects to prepare the primary master because it deforms the fibers, especially polymeric fibers, and creates undesirable spacing between fabric lines. Figure 1 and supplementary movie M1 schematically show how a single fiber was used to create planar parallel grooves, cylindrical helices, twisted fiber helices, and combined hierarchical structures. Wrapping a fiber around a plane object is the simplest way to create planar parallel microgrooves. The primary fiber master without additional polymer coating can be used directly to fabricate master templates with a half-circle profile. To prepare wavy structures, a thin layer of PDMS was coated onto the primary fiber master using a spin coater. The fiber-PDMS composite construct was then used for building a poly(ethylene glycol)-diacrylate (PEGDA) master and subsequently a PDMS replica (Figure 1a,b). The fiber diameter is an important parameter to adjust the groove depth and width. PDMS viscosity and spin speed determine how gaps between fibers are filled to make wavy structures and can be adjusted to modify the waviness of the surface.

Controlled generation of curved or of helical 3D surfaces is of high interest in tissue engineering. Most organs and tissues consist of hierarchically arranged curved shapes. For instance, blood vessels, intestine, esophagus, and trachea have a luminal or cylindrical shape. In order to reconstruct such tissues in vitro, cells and matrix need to be guided to align and assemble in the desired volumetric shape with typical diameters between a few micrometers (small blood vessels) up to several millimeters (large vessels and other structures). The flexibility of FAM enables us to create unconventional geometrical volumes, which have been difficult to microfabricate before. We constructed parallel groove micropatterns inside a small PDMS tube by wrapping a fiber around a syringe needle. After curing the PDMS around the construct, the needle was ejected and the thread removed from the resulting tube (Figure 1c, d). For instance, these patterned hollow tubes are suitable as substrates for tissue engineering blood vessels or tracheal tubes. In case of using biodegradable fibers and appropriate fixing or welding methods to fuse the fabric construct, it is possible to directly use fabric templates as tissue scaffold. As an example, layers of aligned smooth muscle cells could be grown in the lumen to form a contractile vessel wall followed by endothelial cell seeding. Another useful application could be engineering of ring-like muscles (sphincters), which are found in many organs such as the urinary tract[15] or esophagus.

With a slight modification, FAM can also be used to create hierarchical patterned microgrooves. A bundle of 7 nickel threads each with a 100 μm diameter was twisted at the ends, and then the twisted thread was used to prepare a PDMS template which was then seeded with human foreskin fibroblasts (HFFs) (Figure 1e). In Figure 1f the 3D reconstruction of such a construct by confocal microscopy is shown. The twisted nickel threads where then used to create parallel microgrooves by the described method to fabricate more complex hierarchical PDMS templates (Figure 1g). Helically arranged cells and matrix are characteristic of many load-bearing tissues such as bone, tendon, intervertebral discs or vessel walls due to their highly optimized mechanical performance. In another attempt, we created a helically micropatterned hollow tube in PDMS by wrapping a bundle of nylon threads with a helical angle of about 45° around a tube (Figure 1h and Supporting Information Movie M2). The twisting angle of the helix is determined by the number of single fibers in a bundle, and by the tube and thread diameters. To our knowledge, no other easily applicable method has previously been described that allows for fabricating template substrates to direct the growth of such hierarchically organized tissues and to systematically investigate the role of the helical angle for tissue function.

To assess the applicability of FAM for tissue engineering, a sinusoidal wavy PDMS micropattern with wavelength of 200 μm and 40 μm amplitude was created. Another PDMS stamp with square profile (channel-ridge) having the same wavelength and amplitude was created by conventional photolithography to serve as control (Figure S1, Supporting Information). Methacrylated gelatin (GelMA) micropatterned hydrogels were then created by microcontact molding using the prepared stamps (Supporting Information). These hydrogels were used to promote myoblast alignment and differentiation into myotubes. Cells on GelMA hydrogels have the ability to elongate, migrate, and connect with neighboring cells, which is essential for mimicking muscle tissue in vitro.[16] In previous studies, we have shown that GelMA channel-ridge micropatterns promote myoblast alignment and differentiation into thin and long myotubes.[17,18] **Figure 2**a,b. show the fraction of normalized aligned cell nuclei in sinusoidal grooves and channel-ridges with their respective fluorescence microscopy images at day 3 of culture. The graphs show that both patterns induced the alignment of C2C12 myoblasts, and that there was no significant difference in the nuclear alignment between different micropatterns at this stage. Following this, myoblasts were allowed to differentiate into myotubes by changing the culture medium to differentiation medium. After 8 days of culture, we analyzed the orientation angles of the resulting myotubes. Image analysis showed that almost 90% of myotubes on the wavy grooves were aligned, while only 60% of myotubes were aligned on the channel-ridge micropattern ($p < 0.05$) (Figure 2c–f).

DOI: 10.1002/smll.201400263

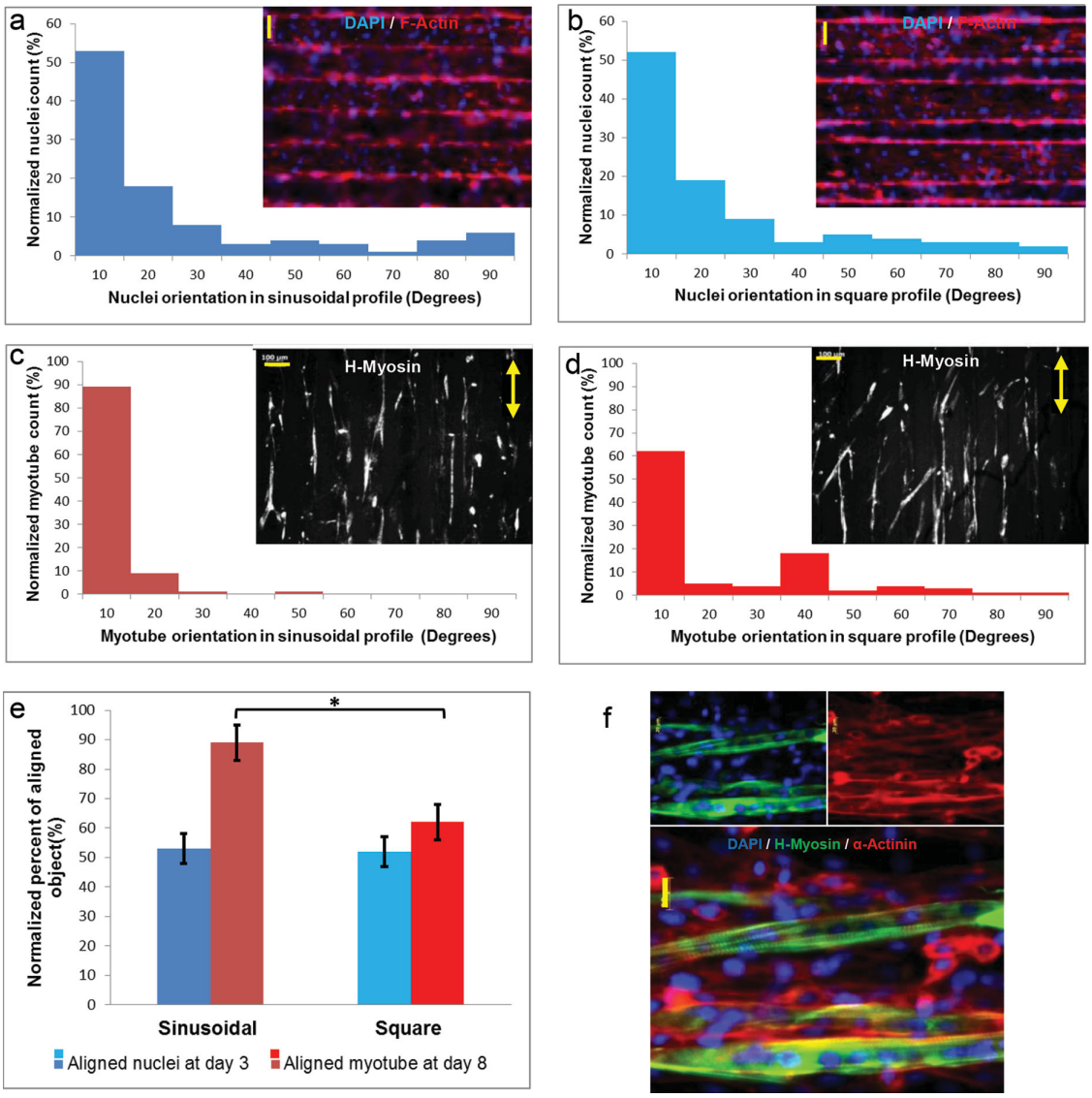

Figure 2. Myoblast and myotube alignment on microgrooves. Alignment of myoblasts on 20% GelMA a) 200 µm wavelength sinusoidal profile microgrooves and b) 200 µm square profile microgrooves. Representative pictures of DAPI/F-actin staining of the samples are shown in the corner of each histogram. Myotube alignment at day 8 of culture on 20% GelMA hydrogels with c) sinusoidal profile microgrooves and d) square profile microgrooves and histograms of the relative orientation show the alignment of myotubes. Representative pictures of anti-myosin heavy chain staining are shown in the corner of each histogram while the yellow arrow shows the direction of the micropattern. e) The comparison of myotubes alignment between both micropatterns shows that the sinusoidal pattern obtained with our fiber technique is much more efficient in directing myotubes (*$p < 0.05$) while cell nuclei alignment at day 3 does not show a difference between the two patterns. f) Immunofluorescence images of myosin heavy chains (green) and cell nuclei (blue) and α-actinin (red for myotubes cultured on the wavy microgrooved GelMA hydrogel on day 8 of culture. Scale bars, 100 µm (a–d), 20 µm (f).

To study the role of curvature in cell contact guidance, arrays of semi-cylindrical structures were made by FAM as presented in Figure 1 using nylon threads. Fibers with a diameter of 180, 250, 400, and 500 µm were selected for the construction of the templates. HFFs were then seeded on these semi-cylindrical microgrooves in culture medium that included fluorescently-labeled fibronectin (Fn) for visualization of fibrillar Fn in the extracellular matrix (ECM). In addition, cells were fixed and nuclei and actin cytoskeleton were stained for future analysis (Supporting Information). **Figure 3** g shows that HFFs clearly deposit fibrillar Fn and align along the pattern axis over the semi-cylindrical features. Analysis of cell nuclei alignment showed that cells aligned more on curved constructs compared to the flat control surface (Figure 3f). Patterns with smaller curvature showed stronger cell alignment, but even the smallest curvature which was made by fibers with a diameter of 500 µm still had an impact on cell alignment compared to the flat control surface.

By filling spaces between fibers with a thin layer of a viscous polymer, it is possible to make continuous wavy grooves and glue the structures to make free standing scaffolds. Coating with polymer not only fills the voids between the fibers, but it can also fills defects or features on individual fibers which might remain from fiber processing and thereby build a smooth surface for cell studies. The replica molding

small 2014,
DOI: 10.1002/smll.201400263

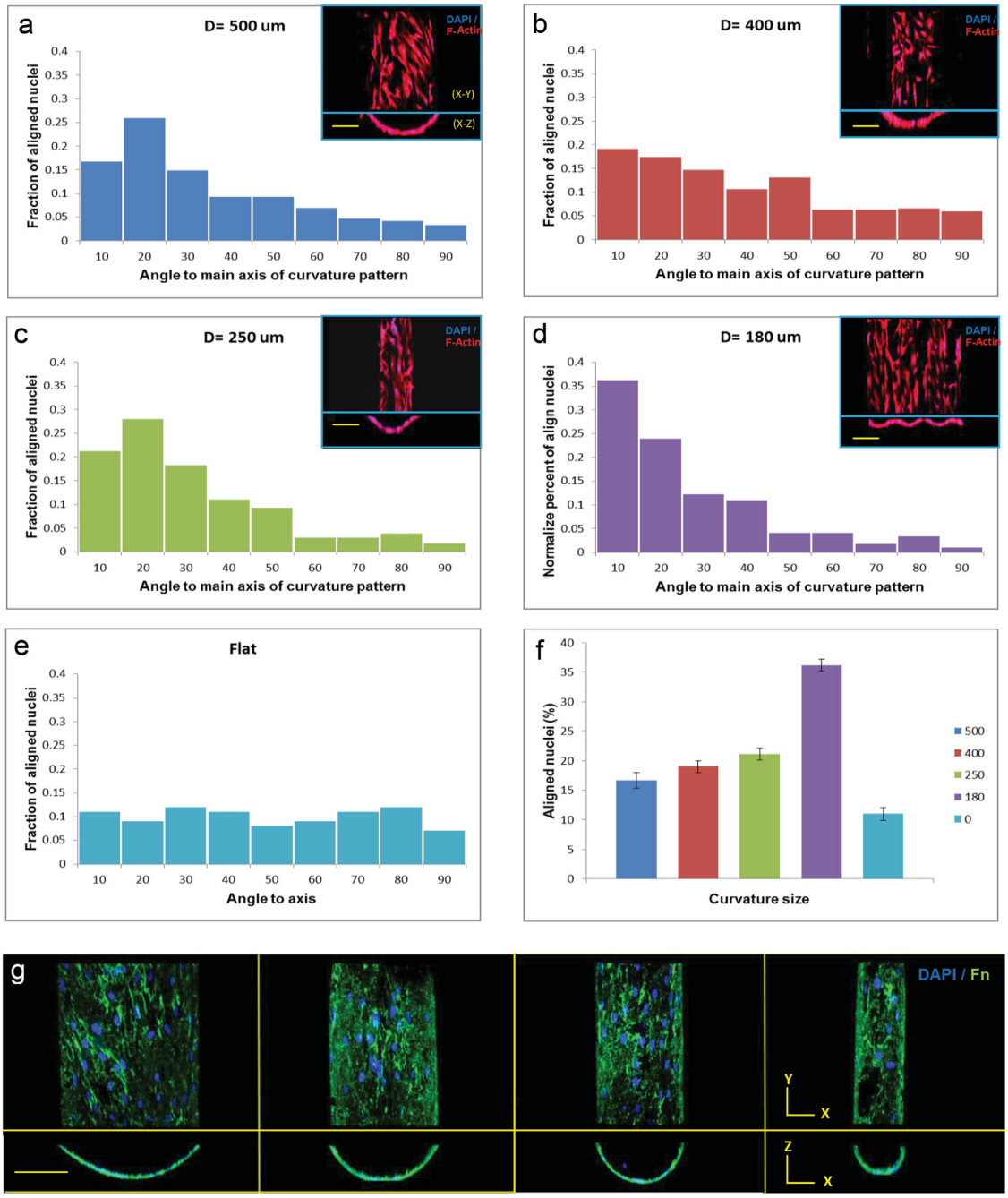

Figure 3. Fibroblast alignment on curved microgrooves. a–e) Histograms of the relative orientation show fibroblast alignment in microgrooves of different curvatures and on a flat surface. f) The comparison of fibroblast alignment shows that, while all microgrooves direct cell alignment, the smallest curvature has the largest effect ($p < 0.01$) compared to flat and other microgrooved surfaces. Representative 3D Z projection pictures along *z* and *y* axis of DAPI/F-actin staining of the samples are shown in the corner of each histogram. g) 3D projection of stacks along *z* and *y* axis confocal microscopy images shows the arrangement of fibroblasts over the curved grooves. Blue represents cell nuclei (DAPI), green is Alexa Fluor-488 fibronectin, and red represents F-actin (Phalloidin). Scale bars 200 μm.

described in Figure 1 also allows creating either concave or convex mesoscale curvature which is known to have different effects on cell behavior.[19] Curvature on sub-micrometer length scales was shown to impact stem cell fate and neural progenitor cell differentiation,[20] but the interaction of cells and curvature on larger scales was rarely studied because of difficulties in manufacturing such curved substrates. It is expected that, while microscopic curvature determines single cell behavior,[21] macroscopic curvature in contrast impacts the interaction of cells, thereby facilitating the formation of functional multicellular structures and large-scale matrix organization. In this paper, we studied collective cell contact guidance on curved grooves and compared them to conventional lithographic square profile grooves. Previous studies have shown that myoblasts were almost fully aligned in small wavy grooves of less than 10 μm wavelength, whereas large sinusoidal grooves have not been tried before due to fabrication difficulties.[5,7] Here we can show that large

DOI: 10.1002/smll.201400263

sinusoidal grooves are superior in myotube alignment compared to their square profile counterparts, thus highlighting the advantage of such constructs to improve cellular alignment, particularly in highly organized and aligned tissues such as muscle. Interestingly, the difference was only significant after myotube fusion (day 8), but not at early timepoints (day 3). A possible explanation could be that myoblasts on curved grooves tend to migrate towards the lowest regions of the grooves, whereas they equally distribute over the flat surfaces of the square grooves, as evident from the images in Figure 2, leading to more likely end-to-end alignment and subsequent fusion on curved vs. square grooves.

It is also well known that other cell types such as fibroblasts, smooth muscle cells, neurons, and, endothelial cells are able to respond to surface topography. While the radius of curvature is expected to play a role for tissue alignment, it has so far been difficult to quantify due to the lack of reproducible fabrication methods. We used our newly developed method to show a relationship between curvature and cell guidance on curved grooves, confirming past studies over single glass fibers.[14] Our investigation adds evidence to the emerging paradigm that cells can collectively feel topography and curvature at length scales of hundreds of micrometers much larger than their own size.[22]

We did not observe any differences in cell viability when using fibers of different chemical composition. While transfer of surface chemical properties from the fiber to the mold cannot be excluded, any such chemical imprint by the fibers could in principle be removed by including appropriate washing steps for the mold and/or the final substrate. Due to the high fidelity of the molding process, any microscopic surface topography of the fibers is also transferred to the mold. Recent advances in fabrication nanoscale fibers of meter scale length will make it possible to scale down the technique to the nanometer range. Conductive twisted hybrid carbon nanotube-graphene[23] could be used to study electroactive tissues such as muscle and neural tissues,[24] and micro-nano-topographies can be included using advanced yarns to improve cell contact guidance.[25] If a smooth surface is desired, the PDMS spinning process explained in the methods section can be used to cover smaller structures.

We have demonstrated that helically patterned tubes can template the alignment of cells and ECM into curved structures on larger scales, which would be expected but has previously been difficult to achieve. The FAM approach is thus prone to open new doors for biological and biomedical studies leading to a better understanding of the mechanisms behind guiding collective cell behavior via topological features that ultimately gives rise to the formation of complex, hierarchical tissue architecture. Examples are the helical hierarchical architecture of heart,[26] the helical arrangement of collagen in the osteons of cortical bone,[1] the large-scale organization of neural and muscle tissues,[17,27] the helical organization of vessel walls,[28] sphincters in the gastrointestinal and urinary tract,[15,29] and the collagen fibers in intervertebrate discs.[26]

In summary, we present FAM as a simple and versatile method to fabricate curved patterns and parallel grooves on planar or curve surfaces, as well as helical patterns in tubes, for guiding and organizing cells and their matrix. As a proof-of-concept, we aligned myoblasts and myotubes in curved parallel microgrooves and showed their superiority for myotube alignment compared to conventional photolithography-based microgrooves. Fibroblast alignment on differently curved grooves was compared, and the results showed that even grooves as large as 500 μm in diameter are able to affect cell direction compared to flat surfaces. Patterned tubes with fine parallel or helical curved grooves are hard to make with current technologies, and based on our knowledge, FAM is by far the simplest among all microfabrication strategies available for this purpose. Besides basic cell biological questions, this method can be applied to guide the assembly of anisotropic tissues with important applications in the area of vascular, muscular and neural tissue engineering. Also other material science applications can be envisioned.

Experimental Section

For making primary master structures, fibers with different diameter were selected and then manually wrapped around a solid object of interest (Supporting Information Movie M1). At this step, any type of object can be used, such as glass slides, tubes, or needles. Accurate groove width of the final construct is achieved by wrapping the fiber without leaving any gaps between turns. This construct can be used directly as a master for replica molding, but it is also possible to adjust feature sizes and geometry by spin coating an additional polymer layer over the fiber array. In this study, we spin-coated PDMS onto the master, removed excess PDMS and then cured the PDMS layer to fill the grooves between the fiber arrays, which results in sinusoidal wavy features (Figure 1a,d,e). This fiber-PDMS master (primary master) was then used to create a PEGDA permanent master as previously described.[30] Details of the fabrication procedure, including movies, can be found in the supplementary information.

Supporting Information

Supporting Information is available from the Wiley Online Library or from the author. Supporting Text SI: detailed description of all materials and experimental procedures. Supporting Figure S1: Cross-sectional schematic of different grooved profile. Supporting Movie M1: visual demonstration of the fiber wrapping procedure. Supporting Movie M2: visual demonstration of replica molding and needle/thread ejection.

Acknowledgements

This work was supported by World Premier International Research Center Initiative (WPI), MEXT, Japan. Parts of the research leading to these results have received funding by the EU Seventh Framework Program (FP7/2007–2013) under grant agreement no. 327065 (P.K.). Funding from the ETH Zurich is gratefully acknowledged

DOI: 10.1002/smll.201400263

(V.V). V.H greatly acknowledges Dr. Kuniaki Nagamine and Mr. Yuichiro Ido for their assistance to take the SEM images.

[1] P. Fratzl, R. Weinkamer, *Prog. Mater. Sci.* **2007**, *52*, 1263.
[2] a) P. Kollmannsberger, C. Bidan, J. Dunlop, P. Fratzl, *Soft Matter* **2011**, *7*, 9549; b) S. C. Cowin, *Annu. Rev. Biomed. Eng.* **2004**, *6*, 77.
[3] a) C. J. Bettinger, R. Langer, J. T. Borenstein, *Angew. Chem., Int. Ed.* **2009**, *48*, 5406; b) V. Vogel, M. Sheetz, *Nat. Rev. Mol. Cell Biol.* **2006**, *7*, 265.
[4] a) B. Trappmann, J. E. Gautrot, J. T. Connelly, D. G. Strange, Y. Li, M. L. Oyen, M. A. C. Stuart, H. Boehm, B. Li, V. Vogel, *Nat. Mater.* **2012**, *11*, 642; b) D. Qin, Y. Xia, G. M. Whitesides, *Nat. Protocols* **2010**, *5*, 491; c) A. Khademhosseini, R. Langer, J. Borenstein, J. P. Vacanti, *Proc. Natl. Acad. Sci. USA* **2006**, *103*, 2480; d) E. Kang, Y. Y. Choi, S. K. Chae, J. H. Moon, J. Y. Chang, S. H. Lee, *Adv. Mater.* **2012**, *24*, 4271.
[5] M. T. Lam, S. Sim, X. Zhu, S. Takayama, *Biomaterials* **2006**, *27*, 4340.
[6] A. Mathur, S. W. Moore, M. P. Sheetz, J. Hone, *Acta Biomater.* **2012**, *8*, 2597.
[7] a) X. Y. Jiang, S. Takayama, X. P. Qian, E. Ostuni, H. K. Wu, N. Bowden, P. LeDuc, D. E. Ingber, G. M. Whitesides, *Langmuir* **2002**, *18*, 3273; b) M. T. Lam, Y.-C. Huang, R. K. Birla, S. Takayama, *Biomaterials* **2009**, *30*, 1150.
[8] C. Polzin, S. Spath, H. Seitz, *Rapid Prototyping Journal* **2013**, *19*, 37.
[9] a) J. Ren, L. Li, C. Chen, X. Chen, Z. Cai, L. Qiu, Y. Wang, X. Zhu, H. Peng, *Adv. Mater.* **2013**, *25*, 1224; b) K. Wang, Q. Meng, Y. Zhang, Z. Wei, M. Miao, *Adv. Mater.* **2013**, *25*, 1494.
[10] R. He, T. D. Day, M. Krishnamurthi, J. R. Sparks, P. J. A. Sazio, V. Gopalan, J. V. Badding, *Adv. Mater.* **2013**, *25*, 1460.
[11] M. D. Lima, N. Li, M. Jung de Andrade, S. Fang, J. Oh, G. M. Spinks, M. E. Kozlov, C. S. Haines, D. Suh, J. Foroughi, S. J. Kim, Y. Chen, T. Ware, M. K. Shin, L. D. Machado, A. F. Fonseca, J. D. W. Madden, W. E. Voit, D. S. Galvão, R. H. Baughman, *Science* **2012**, *338*, 928.
[12] K. Aviss, J. Gough, S. Downes, *Eur Cell Mater* **2010**, *19*, 193.
[13] T. Neumann, S. D. Hauschka, J. E. Sanders, *Tissue Eng.* **2003**, *9*, 995.
[14] Y. Rovensky, V. Samoilov, *J. Cell Sci.* **1994**, *107*, 1255.
[15] K.-D. Sievert, B. Amend, A. Stenzl, *Eur. Urol.* **2007**, *52*, 1580.
[16] a) H. Aubin, J. W. Nichol, C. B. Hutson, H. Bae, A. L. Sieminski, D. M. Cropek, P. Akhyari, A. Khademhosseini, *Biomaterials* **2010**, *31*, 6941; b) J. W. Nichol, S. T. Koshy, H. Bae, C. M. Hwang, S. Yamanlar, A. Khademhosseini, *Biomaterials* **2010**, *31*, 5536; c) S. Ostrovidov, V. Hosseini, S. Ahadian, T. Fujie, S. P. Parthiban, M. Ramalingam, H. Bae, H. Kaji, A. Khademhosseini, *Tissue Eng. Part B* **2013**.
[17] V. Hosseini, S. Ahadian, S. Ostrovidov, G. Camci-Unal, S. Chen, H. Kaji, M. Ramalingam, A. Khademhosseini, *Tissue Eng. Part A* **2012**, *18*, 2453.
[18] J. Ramon, S. Ahadian, R. Obregon, G. Camci-Unal, S. Ostrovidov, V. Hosseini, H. Kaji, K. Ino, H. Shiku, A. Khademhosseini, *Lab Chip* **2012**, *12*, 2959.
[19] J. Y. Park, D. H. Lee, E. J. Lee, S.-H. Lee, *Lab Chip* **2009**, *9*, 2043.
[20] a) S. Ankam, M. Suryana, L. Y. Chan, A. A. Kywe Moe, B. K. Teo, J. B. Law, M. P. Sheetz, H. Y. Low, E. K. Yim, *Acta Biomater.* **2012**, *9*, 4535. b) A. A. K. Moe, M. Suryana, G. Marcy, S. K. Lim, S. Ankam, J. Z. W. Goh, J. Jin, B. K. K. Teo, J. B. K. Law, H. Y. Low, E. L. K. Goh, M. P. Sheetz, E. K. F. Yim, *Small* **2012**, *8*, 3050.
[21] a) G. Miquelard-Garnier, J. A. Zimberlin, C. B. Sikora, P. Wadsworth, A. Crosby, *Soft Matter* **2010**, *6*, 398; b) J. A. Sanz-Herrera, P. Moreo, J. M. García-Aznar, M. Doblaré, *Biomaterials* **2009**, *30*, 6674; c) J. Knychala, N. Bouropoulos, C. Catt, O. Katsamenis, C. Please, B. Sengers, *Ann. Biomed. Eng.* **2013**, 1.
[22] a) C. M. Bidan, K. P. Kommareddy, M. Rumpler, P. Kollmannsberger, Y. J. Bréchet, P. Fratzl, J. W. Dunlop, *PLoS One* **2012**, *7*, e36336; b) M. Rumpler, A. Woesz, J. W. Dunlop, J. T. van Dongen, P. Fratzl, *J. R. Soc., Interface* **2008**, *5*, 1173.
[23] a) M. K. Shin, B. Lee, S. H. Kim, J. A. Lee, G. M. Spinks, S. Gambhir, G. G. Wallace, M. E. Kozlov, R. H. Baughman, S. J. Kim, *Nat. Commun.* **2012**, *3*, 650; b) H.-P. Cong, X.-C. Ren, P. Wang, S.-H. Yu, *Sci. Rep.* **2012**, *2*, 613.
[24] a) J. Ramon, S. Ahadian, M. Estili, X. Liang, S. Ostrovidov, H. Kaji, H. Shiku, M. Ramalingam, K. Nakajima, Y. Sakka, A. Khademhosseini, T. Matsue, *Sci. Rep.* **2013**, *25*, 4028. b) J. Ramon, S. Ahadian, M. Estili, X. Liang, S. Ostrovidov, H. Kaji, H. Shiku, M. Ramalingam, Y. Sakka, A. Khademhosseini, T. Matsue, *Adv. Mater.* **2013**, *25*, 4028.
[25] Y. Liu, T. Wang, Y. Huan, Z. Li, G. He, M. Liu, *Adv. Mater.* **2013**, *25*, 5875.
[26] N. L. Nerurkar, D. M. Elliott, R. L. Mauck, *Journal of biomechanics* **2010**, *43*, 1017.
[27] M. Georgiou, S. C. J. Bunting, H. A. Davies, A. J. Loughlin, J. P. Golding, J. B. Phillips, *Biomaterials* **2013**, *34*, 7335.
[28] J. A. Rhodin, *Compr. Physiol.* **2011**, Supp 71-35.
[29] J. Tan, C. Chua, K. Leong, K. Chian, W. Leong, L. Tan, *Biotechnol. Bioeng.* **2012**, *109*, 1.
[30] C. M. Huwang, W. Y. Sim, S. H. Lee, A. M. Foudeh, H. Bae, S. Lee, A. Khademhosseini, *Biofabrication* **2010**, *2*, 045001.

Received: January 29, 2014
Revised: May 22, 2014
Published online: